COMPARISON OF THE SULFIDE-BEARING HAYABUSA PARTICLES RB-CV-0234 AND RB-QD04-0039 TO LL CHONDRITE SULFIDES. D. L. Schrader[1] and T. J. Zega[2], [1]*Center for Meteorite Studies, School of Earth and Space Exploration, Arizona State University, Tempe, AZ 85287, USA (devin.schrader@asu.edu),* [2]*Lunar and Planetary Laboratory, University of Arizona, Tucson, Arizona 85721, USA (tzega@lpl.arizona.edu).*

Introduction: The compositions, textures, and crystal structures of sulfides can be used to constrain oxygen fugacity of formation, shock stage, and aqueous-, thermal-, and cooling-histories of their host rocks [e.g., 1–6]. The most abundant sulfides in extraterrestrial samples are the pyrrhotite group [$(Fe,Ni,Co,Cr)_{1-x}S$], which can occur with pentlandite [$(Fe,Ni,Co,Cr)_{9-x}S_8$], FeNi metal, and oxides [e.g., 7,8]. The pyrrhotite-group sulfides are largely non-stoichiometric, where x in $Fe_{1-x}S$ varies between 0 and 0.125, and occur in different polytypes sensitive to thermodynamic conditions. Pyrrhotites can be described with a NiAs-type structure, where polytypes are described NC; the value of N designates the multiple of the superstructure in the c-axis dimension [e.g., 5]. The stoichiometric end members are 2C (troilite; FeS, hexagonal) and 4C (Fe_7S_8, monoclinic) pyrrhotite. There are also pyrrhotites of intermediate compositions with $0<x<0.125$, all of which are hexagonal, and include the non-integral NC-pyrrhotites and the integral 5C (Fe_9S_{10}), 6C ($Fe_{11}S_{12}$), and 11C ($Fe_{10}S_{11}$) pyrrhotites [e.g., 9–11].

Geothermometry of pyrrhotite-pentlandite intergrowths in meteorites shows that most formed via primary cooling from high temperature or thermal metamorphism [e.g., 7,8,12]. Sulfides in the LL4 to LL6 chondrites typically equilibrated between 600 and 500°C, consistent with formation during cooling after thermal metamorphism [8]. However, geothermometry of pyrrhotite-pentlandite intergrowths from an LL5–6 impact melt-breccia indicated that the sulfides were annealed at ≤230°C, likely after an impact event [7]. In comparison, analyses of Hayabusa particles have identified asteroid 25143 Itokawa as LL4 to LL6 chondrite material (~10% LL4 and ~90% LL5 to LL6) [e.g., 13–16] that was thermally metamorphosed between ~780 and 840°C [13]. Itokawa particles were found to record shock stages between S2 and S4, with most particles around S2 [17,18]. Sulfides in Hayabusa particles [e.g., 13,19,20] may record additional and/or complementary information on the formation conditions of Itokawa. Our goal is to further constrain the formation and alteration conditions of asteroid Itokawa via comparison of sulfide-bearing Hayabusa particles to LL3 through LL6 chondrite sulfides.

Samples and Analytical Procedures: We were allocated sulfide-bearing Itokawa samples RB-CV-0234 and RB-QD04-0039 from the JAXA collection, which were provided as intact grains measuring 25.9 μm and 53 μm in diameter, respectively. We embedded the grains in low-viscosity epoxy and prepared them with the hybrid ultramicrotome-focused ion beam (FIB) technique developed by [19], previously used on other Hayabusa particles [21,22]. We made ultramicrotome sections of the first few hundred nm of the grains and left the bulk for analysis and preparation using FIB. Electron-transparent cross sections of the particles were created using the FEI Helios NanoLab 660 focused-ion-beam-scanning electron microscope (FIB-SEM) at the University of Arizona (UAz). In addition, we also extracted a FIB section of a pyrrhotite-pentlandite grain from Chelyabinsk ASU1801_22_C1 (LL5, S5). X-ray element maps and high-resolution images of the sulfides were obtained with the FIB-SEM prior to extraction of ~10 × 10 μm sections, which were then thinned to electron transparency (<100 nm) following the methods of [23]. The FIB sections were then analyzed using the 200 keV aberration-corrected Hitachi HF5000 scanning transmission electron microscope (TEM) at UAz.

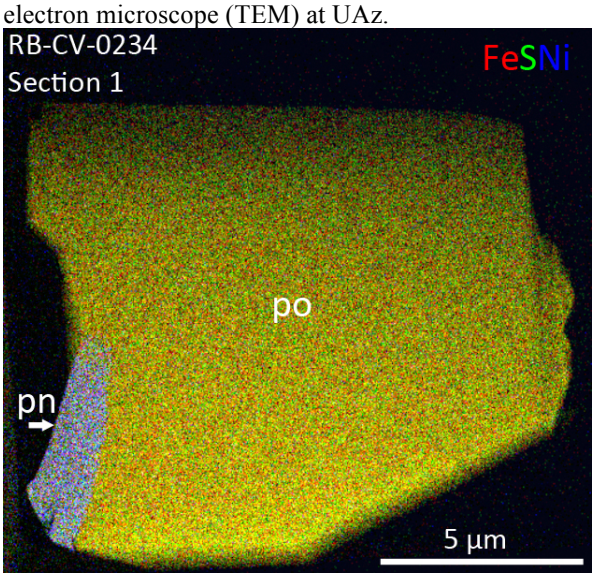

Figure 1. Composite TEM X-ray element map of RB-CV-0234 FIB Section 1; po = pyrrhotite and pn = pentlandite.

Results: *RB-CV-0234:* X-ray maps of the surface of the microtomed particle reveal that it is composed entirely of pyrrhotite. However, X-ray element maps of the extracted FIB section, determined via TEM analysis, show a single grain of pyrrhotite and a buried pentlandite grain (4.8 × 1.3 μm; Fig. 1). Selected-area electron-diffraction (SAED) patterns of the pyrrhotite and pentlandite grains at the same goniometer tilt angle index to the [110] zone axis for both 2C pyrrhotite (troilite) and pentlandite.

RB-QD04-0039: X-ray maps of the surface of the microtomed particle show that it is primarily composed of olivine that displays planar fractures, with minor amounts of low-calcium pyroxene, plagioclase, and a single grain of pyrrhotite (5.5 × 2.7 μm). TEM analysis revealed the FIB section contains olivine and at least two distinct grains (indicated by arrows in Fig. 2) of 2C pyrrhotite that are each polycrystalline on sub-micron scales.

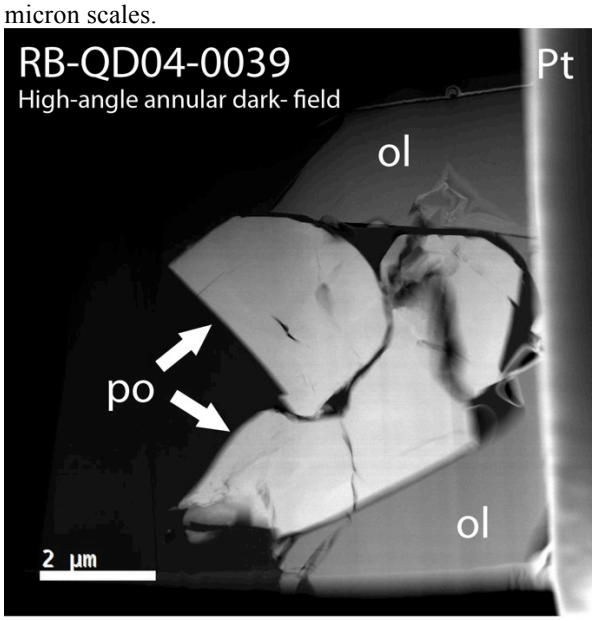

Figure 2. RB-QD04-0039 contains two grains of polycrystalline pyrrhotite (po), in contact with olivine (ol).

Chelyabinsk (LL5, S5): An X-ray map shows that the FIB section is dominated by pyrrhotite and contains a grain of pentlandite. TEM analysis revealed each grain consists of polycrystalline 2C pyrrhotite and polycrystalline pentlandite (on ~micron scales).

Discussion: *RB-CV-0234:* The preliminary results from the FIB section from RB-CV-0234 are most consistent with it being a sulfide from an LL6, S2 chondrite, as it is similar to sulfides from Saint-Séverin studied by [24]. We infer this because, based on results from the LL3 to LL6 chondrite sulfides we have studied via FIB-TEM [24,25,this study], only sulfide grains in Saint-Séverin (LL6, S2 [26]) contain a similar pentlandite/pyrrhotite morphology (i.e., blocky pentlandite in pyrrhotite) and 2C pyrrhotite (troilite) with pentlandite [24]. The other LL chondrites we studied contained either a distinct morphology (e.g., pentlandite lamellae), multiple polytypes of pyrrhotite, and/or polycrystalline pyrrhotite [24,25,this study]; perhaps indicating higher degrees of shock as troilite in ordinary chondrites is known to display shock indicators, such as fizzed and polycrystalline troilite [e.g., 6].

RB-QD04-0039: The preliminary results from the FIB section from RB-QD04-0039 are most consistent with it being a sulfide from an LL5, S5 chondrite, as it is similar to the sulfides from Chelyabinsk (LL5, S5) analyzed here. We infer this because of the LL3 to LL6 chondrite sulfides we have studied via FIB-TEM [24,25,this study], only Chelyabinsk contains polycrystalline 2C pyrrhotite. This is consistent with RB-QD04-0039 containing; (1) polycrystalline troilite, indicating ≥S3 according to the scheme of [6]; and (2) olivine with planar fractures, indicating ≥S3 by the scheme of [27].

These conclusions are consistent both with the petrographic types represented in Hayabusa particles (10% LL4 and 90% LL5 to LL6 [13,15,16]) and the observed shock stages of Hayabusa samples (S2–4; [17,18]). FIB section extractions from new LL chondrites and additional sections from RB-CV-0234 are in progress. TEM analyses of these new sections will allow us to verify these conclusions and investigate if the sulfide from RB-CV-0234 contains any evidence of space weathering [e.g., 20].

References: [1] Arnold R. G. (1967) *Can. Min.* 9, 31. [2] Kissin S. A. and Scott S. D. (1982) *Econ. Geol.* 77, 1739. [3] Raghavan V. (2004) *J. Phase Equilib.* 25, 373. [4] Wang H. et al. (2006) *J. Sulfur Chem.* 27, 1. [5] Harries D. and Langenhorst F. (2013) *MAPS* 48, 879. [6] Bennet M. E. and McSween Jr. H. Y. (1996) *MAPS* 31, 255. [7] Jamsja N. and Ruzicka A. (2010) *MAPS* 45, 828. [8] Schrader D. L. et al. (2016) *GCA* 189, 359. [9] Morimoto N. et al. (1975) *Econ. Geo.* 70, 824. [10] Wang H. et al. (2006) *J. Sulfur Chem.* 27, 1. [11] Harries D. et al. (2011) *Am. Min.* 96, 716. [12] Schrader D. L. et al. (2015) *MAPS* 50, 15. [13] Nakamura T. et al. (2011) *Science* 333, 1113. [14] Noguchi T. et al. (2014) *EPS* 66, 124. [15] Tsuchiyama A. et al. (2011) *Science* 333, 1125. [16] Tsuchiyama A. et al. (2014) *Meteorit. Planet. Sci.* 49, 172. [17] Noguchi T. et al. (2011) *Science* 333, 1121. [18] Zolensky M. E. et al. 2012. *LPS XLIII* Abstract #1477. [19] Berger E. L. and Keller L. P. (2015) *Microscopy Today* 23, 18. [20] Harries D. and Langenhorst F. (2014) *EPS* 66, 163. [21] Zega T. J. (2017) *LPS XLVIII* Abstract #3037. [22] Thompson M. S. (2017) *LPS XLVIII* Abstract #2358. [23] Zega T. J. et al. (2007) *MAPS* 42, 1373. [24] Schrader D. L. and Zega T. J. (2017) *80th MetSoc.* Abstract #6347. [25] Schrader D. L. and Zega T. J. (2018) *LPS XLIX* Abstract #2621. [26] Rubin A. E. (2004) *GCA* 68, 673. [27] Stöffler D. et al. (1991) GCA 55, 3845.

Acknowledgements: We thank JAXA for the loan of the Hayabusa particles used in this study, the Smithsonian Institution and ASU Center for Meteorite Studies for the loan of meteorites used in this study, and NASA grant NNX17AE53G (DLS PI, TJZ Co-I) for funding this research.